MOLECULAR AND CELLULAR BIOLOGY, Apr. 2009, p. 1707–1718 Vol. 29, No. 7
0270-7306/09/$08.00+0 doi:10.1128/MCB.01184-07

Key Role for Activin B in Cellular Transformation after Loss of the von Hippel-Lindau Tumor Suppressor▽†

Ingrid Wacker,[1] Martin Sachs,[1] Karl Knaup,[1] Michael Wiesener,[1] Jörg Weiske,[2] Otmar Huber,[2]‡ Ziya Akçetin,[3] and Jürgen Behrens[1]*

Nikolaus Fiebiger Center, University Erlangen-Nürnberg, Glückstr. 6, 91054 Erlangen, Germany[1]; Department of Laboratory Medicine and Pathobiochemistry, Charité-Universitätsmedizin Berlin, Campus Benjamin Franklin, Hindenburgdamm 30, 12200 Berlin, Germany[2]; and Department of Urology, Namik Kemal University, Tekirdag, Turkey[3]

Received 3 July 2007/Returned for modification 8 October 2007/Accepted 10 January 2009

The von Hippel-Lindau tumor suppressor gene (VHL) is mutated in clear cell renal cell carcinomas (RCC), leading to the activation of hypoxia-inducible factor (HIF)-mediated gene transcription. Several VHL/HIF targets, such as glycolysis, angiogenesis, cell growth, and chemotaxis of tumor cells, have been implicated in the transformed phenotype of RCC-regulating properties. Here, we show that VHL suppresses key features of cell transformation through downregulation of the HIF-dependent expression of activin B, a member of the transforming growth factor β superfamily. Activin B expression is repressed by restoration of VHL in VHL-deficient RCC cells and upregulated by hypoxia. RCC tumor samples show increased expression of activin B compared to that in the normal kidney. VHL increases cell adhesion to the extracellular matrix, promotes cell flattening, and reduces invasiveness. These effects are completely phenocopied by RNA interference-mediated knockdown of activin B and reverted by treatment with recombinant activin B. Finally, knockdown of activin B reduces tumor growth of RCC cells in nude mice. Our data indicate that activin B is a key mediator of VHL/HIF-induced transformation in RCC.

Mutations of the von Hippel-Lindau tumor suppressor gene (VHL) occur in the majority of sporadic clear cell renal cell carcinomas (RCC) and also in the familial forms of RCC associated with the von Hippel-Lindau hereditary cancer syndrome (16). The VHL protein acts as part of an E3 ligase complex to trigger ubiquitination and subsequent proteasomal degradation of hypoxia-inducible factor 1 (HIF-1) and HIF-2 transcription factors in an oxygen-dependent manner. VHL associates with HIFs after their hydroxylation at specific prolyl residues in the presence of oxygen. Under hypoxic conditions, hydroxylation is prevented, leading to the stabilization of HIFs, which can activate target genes by binding to specific promoter elements (29). VHL mutations associated with RCC abolish the capacity of VHL to induce degradation of HIF and thereby lead to constitutive stabilization of HIFs and target gene expression, even under normoxic conditions (16, 29, 30).

There is strong evidence that inappropriate activation of HIF-dependent gene expression due to the loss of VHL is the main cause of RCC (17, 23). Moreover, activation of HIF targets probably also plays a role in other tumor types, which are exposed to low oxygen tension as a consequence of inadequate blood supply. The inactivation of VHL leads to HIF-dependent expression of a broad spectrum of target genes with a potential role in tumorigenic transformation. Among these are glycolytic enzymes, which may support anaerobic tumor growth, angiogenic factors such as vascular endothelial growth factor, growth factors and receptors such as transforming growth factor α (TGFα) and c-Met, and the CXCR4 chemokine receptor, which could aid in the chemotaxis of metastatic tumor cells (29).

Several studies have shown that the loss of VHL can induce cell motility and invasiveness, which are important parameters of cell transformation (18, 26, 27). Moreover, hypoxia suffices to induce invasiveness of human tumor cell lines (19). Lysyl oxidase activity, which can restructure extracellular matrix (ECM), was shown to be required for hypoxia-induced invasiveness of several tumor cell lines (10). Recent findings also show that the E-cadherin gene is downregulated in VHL-deficient cells, which could lead to the loss of epithelial cell junctions and allow cell migration (11, 13, 20). Thus, VHL/HIF might control invasion and metastasis by regulating various molecular components.

Activin B is a member of the TGFβ family of secreted proteins, which stimulates Smad and Map kinase signaling pathways after binding and activation of specific cell surface receptors. Activin B is a homodimer of two βB subunits encoded by the inhibin βB gene, which are synthesized as larger precursors that are proteolytically processed to the mature form (6, 33). Mice deficient in activin B are viable but show defects in eyelid and mammary gland development (28, 31). Activin B plays a role in wound healing by promoting reepithelization of wounds, a process that depends on signaling to MEK kinase 1 (MEKK1) and involves regulation of genes for ECM remodeling (8, 25, 34, 35). Activin B is related to activin A, which is composed of two βA subunits, and activin AB,

* Corresponding author. Mailing address: Nikolaus Fiebiger Center, University Erlangen-Nürnberg, Glückstr. 6, 91054 Erlangen, Germany. Phone: 49-9131-8529109. Fax: 49-9131-8529111. E-mail: jbehrens@molmed.uni-erlangen.de.

† Supplemental data for this article may be found at http://mcb.asm.org/.

‡ Present address: Institute for Biochemistry, University of Jena, Nonnenplan 2, 07743 Jena, Germany.

▽ Published ahead of print on 21 January 2009.

which is a heterodimer of the βA and the βB chain. Further members of the family are inhibins, which are composed of either βA or βB together with the inhibin α subunit. Interestingly, TGFβ mRNA and protein levels were shown to be repressed by VHL (1).

In this study, we show that VHL can suppress the invasiveness of RCC cells and increase adhesion to the ECM by downregulating activin B. Loss of VHL or hypoxic conditions induce activin B expression in a HIF-dependent manner, which is required and sufficient for triggering cellular invasiveness and decreasing cell matrix interactions of RCC cells. Our data suggest that activin B signaling is a potential target for therapeutic interventions of RCC and other tumor types associated with hypoxic conditions.

MATERIALS AND METHODS

Cell culture. 786.0, 786.0 VHL+ (15), RCC4, RCC4 VHL+ (24), and HCT116 cell lines were cultured in Dulbecco's modified Eagle's medium (DMEM) supplemented with 10% fetal calf serum (FCS) and 1% penicillin/streptomycin at 37°C in a humidified atmosphere of 10% CO_2. For chemical stabilization of HIF, desferroxamine (DFO; Sigma-Aldrich, Munich, Germany) was solved in phosphate-buffered saline (PBS) and added at a final concentration of 100 mM for 16 h. For hypoxia experiments, cells were cultured for 16 h at 1% O_2 in a hypoxia incubator (Ruskin Company, Kansas City, MO). For activin B experiments, cells were treated with 10 ng/ml of recombinant activin B (R&D Systems, Minneapolis, MN).

RNA interference. Short interfering RNA (siRNA) oligomers were transfected with TransIT-TKO (Mirus, Madison, WI) according to the manufacturer's instructions. The sequence of the siRNAs used were as follows: siRNA against green fluorescent protein (siGFP), 5′-AAGCUACCUGUUCCAUGGCCA-3′, and two sets of siRNAs against HIF-1α and HIF-2α, including si1HIF-1α, 5′-GCCACUUCGAAGUAGUGCUdTdT-3′; si2HIF-1α, 5′-CUGAUGACCAGCAACUUGAdTdT-3′; si1HIF-2α, 5′-GCGACAGCUGGAGUAUGAAdTdT-3′; and si2HIF-2α, 5′-CAGCAUCUUUGAUAGCAGdTdT-3′. For stable knockdown of activin B, 786.0 cells were transfected with 10 μg of the pSUPER sh1-βB plasmid or with the pSUPER sh2-βB plasmid encoding short hairpin RNAs (shRNAs) targeting human activin βB. pSUPER sh1-βB was generated by cloning the annealed oligonucleotides 5′-GATCCCCGTACAACATCGTCAAGCGGTTCAAGAGACCGCTTGACGATGTTGTACTTTTTGGAAA-3′ (shRNA sequence coding strand) and 5′-AGCTTTTCCAAAAAGTACAACATCGTCAAGCGGTCTCTTGAACCGCTTGACGATGTTGTACGGG-3′ into the BglII/HindIII-digested pSUPER vector (5) containing a neomycin resistance cassette. Oligonucleotides used for pSUPER sh2-βB were 5′-GATCCCCCTTCATAGAGCAACCAGTCTTCAAGAGAGACTGGTTGCTCTATGAAGTTTTTGGAAA-3′ (shRNA sequence coding strand) and 5′-AGCTTTTCCAAAAACTTCATAGAGCAACCAGTCTCTCTTGAAGACTGGTTGCTCTATGAAGGGG-3′. pSUPER sh1-βB, pSUPER sh2-βB, and pSUPER as a negative control were transfected using EscortTM IV transfection reagent (Sigma-Aldrich, Munich, Germany) according to the manufacturer's protocol. Clones were selected in DMEM supplemented with 1 mg/ml Geneticin (G418; Invitrogen, Carlsbad, CA). To generate pools, three individual clones of knockdown and control transfectants were combined.

RNA isolation and RT-PCR. Frozen tissues were disrupted with a power homogenizer, and total cellular RNA was isolated using peqGold Trifast reagent (Peqlab, Erlangen, Germany) by following the manufacturer's protocol. Contaminating genomic DNA was enzymatically removed with DNase I, and the total RNA was further purified according to the manufacturer's protocol, by using a total RNA mini kit (Qiagen, Hilden, Germany). For cells in monolayers, the homogenizer and DNase I treatments were omitted. cDNAs were generated by reverse transcriptase reactions using 1 μg of RNA and 2 μl of random hexamer primer (100 pmol/liter). After incubation for 10 min at 70°C, 4 μl of 5× first-strand buffer (Invitrogen, Carlsbad, CA), 2 μl of 0.1 mol/liter dithiothreitol, 1 μl of deoxynucleotide triphosphates (10 mmol/l), 40 U of RNase inhibitor (RNaseOut; Invitrogen, Carlsbad, CA), 200 U of SuperScript II reverse transcriptase (Invitrogen, Carlsbad, CA), and diethyl pyrocarbonate water in a final volume of 20 μl were added, and RNAs were transcribed for 1 h at 37°C. Reverse transcriptase was inactivated at 70°C for 10 min. After reverse transcription, PCR was performed in a 10-μl reaction volume according to standard protocols. The following thermal cycling parameters were used: 30 s at 96°C, 1 min at 58°C, and 30 s at 72°C, with an initial step of 96°C for 2 min and a final step of 72°C for 10 min. Sequences for primers were as follows: activin βB, 5′-CTGAGTACAGTCATTCTGTTGGGCTG-3′ (forward) and 5′-TCTCTCCGACTGACAGGCATTTG-3′ (reverse); Glut-1, 5′-GCGGAATTCAATGCTGATGAT-3′ (forward) and 5′-CAGTTTCGAGAAGCCCATGAG-3′ (reverse); CAIX, 5′-GTCCCAGGACTGGACATATCTCGCA-3′ (forward) and 3′-CATTCAAAGGCTGCGTCGCTC-3′ (reverse); IGFBP3, 5′-ACTTCATGCGCCCGTGGAAT-3′ (forward) and 5′-ATGCGTTGGGATGTCCGGAT-3′ (reverse); HIF-1α, 5′-GGTGACAACTGATCGAAGGAACGT-3′ (forward) and 5′-GCAATGTCTCCATTACCCACCGC-3′ (reverse); HIF-2α, 5′-GAGTCCGAAGCCGAAGCTGAC-3′ (forward) and 5′-GGCTGACTTGAGGTTGACAGTACG-3′ (reverse); and β-actin, 5′-GCCGTCGCCCATCATCAAGT-3′ (forward) and 5′-CCAGATCAGGTGTGTAGCCAATGA-3′ (reverse). Real-time quantitative reverse transcription-PCR (RT-PCR) was carried out using an iCycler (Bio-Rad, Hercules, CA) detection system with Q-PCR Mastermix with Sybr green and Fluorescein Green I (Abgene, Epsom, United Kingdom) by following the manufacturer's instructions.

Western blotting. Confluent cells in six-well plates were lysed in 100 μl buffer (20 mM Tris-HCl [pH 7.4], 150 mM NaCl, 5 mM EDTA, 1% Triton X-100, 1 mM phenylmethylsulfonyl fluoride, 1 mM dithiothreitol) for 10 min on ice. Equal amounts of protein were separated by 5% sodium dodecyl sulfate-polyacrylamide gel electrophoresis. For Western blot analysis from the supernatant, 2.8×10^6 cells were grown in 15-cm^2 plates in serum-free DMEM for 24 h. Conditioned medium was concentrated with Vivaspin 20 columns (Sartorius AG, Göttingen, Germany) and separated on a 10% polyacrylamide gel. Proteins were transferred to Hybond N nitrocellulose membranes (Amersham, Freiburg, Germany). Antibodies against human activin B (clone 146807; R&D Systems, Minneapolis, MN), human HIF-1α (clone H1alpha67; BD Transduction Laboratories, Heidelberg, Germany), human HIF-2α (clone ep190b; Novus Biologicals, Littleton, CO), human β-actin (Sigma-Aldrich, Munich, Germany), and peroxidase-conjugated secondary antibodies (Jackson ImmunoResearch, Cambridgeshire, United Kingdom) were used according to the manufacturers' instructions. Signals were visualized using enhanced-chemiluminescence reagent (PerkinElmer, Rodgau, Germany) and detected by exposure to X-ray film (Kodak, Rochester, NY) or by use of a luminescent image analyzer (LAS-3000; Fuji, Düsseldorf, Germany).

Reporter assays. The −1460 rat activin βB promoter (9) was cloned into pGL3basic (Promega, Madison, WI). A fragment from bp −4121 to −3917 relative to the ATG start codon of the human activin βB was cloned upstream of the rat promoter. HRE1 (ACGTG), HRE2 (GCGTG), and HRE3 (GCGTG) were mutated to AAAAG, GAAAG, and GAAAG, respectively. To evaluate promoter activation, HEK293T cells were seeded at 50,000 cells per 12-well plate and transfected with polyethylenimine with 25 ng Rous sarcoma virus–ß-galactosidase, 50 ng of activin βB promoter constructs, and 25 ng or 50 ng of HIF-1α and HIF-2α expression plasmids. The amount of DNA for each transfection was adjusted by the addition of empty pcDNA3.1 vector. Luciferase activity was measured 24 h after transfection according to standard procedures and normalized to β-galactosidase values.

ChIP. Chromatin immunoprecipitation (ChIP) was performed essentially as described earlier (32). Fifty micrograms of DNA was incubated in 300 μl of radioimmunoprecipitation assay buffer overnight at 4°C, with 2 μg of monoclonal mouse anti-human HIF-1α (clone H1alpha67; BD Transduction Laboratories, Heidelberg, Germany), 2 μg of polyclonal rabbit anti-human HIF-2α (Novus Biologicals, Littleton, CO), or anti-immunoglobulin G (Santa Cruz Biotechnology, Santa Cruz, CA) antibodies from mouse and rabbit as controls. Following precipitation of immune complexes, a 204-bp region of the human activin βB promoter was amplified (94°C for 5 min; 25 cycles of 94°C for 15 s, 61°C for 20 s, and 72°C for 30 s; and a final 2-min extension at 72°C) using the following oligonucleotides: forward, 5′-GGGCCAAGAACTGCACCTG-3′, and reverse, 5′-GGGCTTGCAGAAGTTGGAAG-3′. PCR products were separated by electrophoresis on an 8% polyacrylamide gel and visualized by ethidium bromide staining.

Immunofluorescence microscopy. Cells were fixed with 3% paraformaldehyde for 15 min and permeabilized with 0.5% Triton. After being blocked with 10% FCS in DMEM, cells were stained with anti-integrin β1 (1:200; Southern Biotechnology, Birmingham, AL). Cy2-labeled goat anti-mouse antibody (Jackson ImmunoResearch, Cambridgeshire, United Kingdom) was used to visualize the primary antibody. F-actin (filamentous actin) was stained using tetramethylrhodamine isothiocyanate-labeled phalloidin (Sigma-Aldrich, Munich, Germany). Cell micrographs were obtained by using a charge-coupled-device camera (Visitron, Munich, Germany) and a Zeiss Axioplan 2 imaging microscope (Zeiss, Oberkochen, Germany).

Immunohistochemistry. Deparaffinized sections were pretreated with 0.2% hyaluronidase (Roche, Mannheim, Germany) in PBS for 60 min and subsequently with pronase (2 mg/ml in PBS, pH 7.3; Sigma-Aldrich, Munich, Germany) for 60 min at 37°C. The sections were then left to react at 4°C with a monoclonal mouse anti-human HIF-1α antibody (clone H1alpha67; BD Transduction Laboratories, Heidelberg, Germany) diluted 1:200, were then incubated with a biotinylated donkey anti-mouse secondary antibody (Dianova, Hamburg, Germany) and were visualized by the addition of a complex of streptavidin and biotinylated alkaline phosphatase.

Attachment assay and cell spreading analysis. For attachment assays, 1.5×10^4 cells were allowed to attach to plastic or ECM-coated wells of a 96-well plate. Mouse laminin-1 (20 μg/ml; Santa Cruz Biotechnology, Santa Cruz, CA), human fibronectin (10 μg/ml; Harbor Bioproducts, Norwood, MA), collagen I (5 μg/ml, calf skin type I collagen G; Serva Electrophoresis GmbH, Heidelberg, Germany), and mouse collagen IV (5 μg/ml; gift from Klaus von der Mark) were used as ECM substrates. After 1 h (ECM substrates) or after 20 min (plastic), nonadherent cells were washed away with PBS, and the amount of attached cells was determined with an acidic phosphatase assay (4). For this assay, cells were lysed in 100 μl of lysis buffer (50 mM sodium acetate [pH 5.0], 12 mM *p*-nitrophenylphosphate, and 0.2% Triton X-100) and incubated for 1 h at 37°C. The reaction was stopped with 50 μl of 1 N NaOH per well, and extinction was determined at 405 nm. For analysis of cell spreading, 1.5×10^5 cells were seeded on ECM-coated coverslips and fixed with 3% paraformaldehyde after 1 h. Cell shape was analyzed by bright-field microscopy and immunofluorescence microscopy.

Invasion assay. Calf skin type I collagen G (Serva Electrophoresis GmbH, Heidelberg, Germany) and rat tail type I collagen R (Biochrom AG, Berlin, Germany) were mixed at a ratio of 1:1, 0.1 volume of sodium bicarbonate (22 mg/ml) and 0.1 volume of 10× DMEM were added, and the solution was neutralized with sodium hydroxide. Aliquots of 1.2 ml/well were allowed to gel in six-well culture dishes at 37°C. Tumor cells (5×10^4) were directly seeded in DMEM containing 2% FCS on the collagen surfaces. Cells invading the collagen gel were detected by focusing down into the matrix and quantified daily by counting 20 optical fields per well (3).

Tumor samples. Surgically dissected tissue samples were obtained from 34 patients with RCC after radical nephrectomy at the Department of Urology, Waldkrankenhaus, University of Erlangen-Nürnberg. Informed consent was obtained from patients to use their surgical specimens and clinico-pathological data for research purposes. Part of the tumor sample and the corresponding normal renal tissue was snap-frozen in liquid nitrogen by the surgeon within 2 min after dissection and stored at −80°C.

Xenograft experiments. For xenograft experiments, 5.0×10^6 or 3.0×10^6 cells of the respective 786 clones (clone neo 1 [neo#1], a pool of clones neo#1 to neo#3, clone si1-βB 2 [si1-βB#2], a pool of clones si1-βB#1 to si1-βB#3, as well as a pool of clones si2-βB#1 to si2-βB#3), were resuspended in 200 μl PBS and injected subcutaneously into the flanks of 6-week-old female BALB/c nu/nu mice (Charles River Laboratories, Wilmington, MA). Tumor size was measured once a week with a caliper, and tumor volume was calculated by the following formula: (length × width)2/2. Mice were euthanatized 12 weeks after inoculation.

MTT assay. A 3-(4,5-dimethylthiazol-2-yl)-2,5-diphenyl tetrazolium bromide (MTT) assay (Roche Diagnostics GmbH, Mannheim, Germany) was used to control cytotoxicity and cell viability according to the manufacturer's instructions.

RESULTS

Activin B is upregulated by HIF in VHL-deficient tumor cells. In a DNA microarray analysis comparing gene expression patterns of VHL-deficient RCC cells (786.0 and RCC4) with their VHL-transfected counterparts (786.0 VHL+, RCC4 VHL+), we noticed that activin βB mRNA was downregulated by VHL and reexpressed under hypoxia, results similar to those with known HIF target genes (see Table S1 in the supplemental material). These findings were confirmed by qualitative and quantitative RT-PCR analysis (Fig. 1A). The amount of secreted activin B protein was significantly reduced in the VHL transfectants, and treatment of these cells with the hypoxia-mimetic substance DFO induced activin B (Fig. 1B). Activin B was not altered by hypoxia in the VHL-deficient 786.0 and RCC4 cells, indicating that upregulation is HIF mediated and not hypoxia mediated (Fig. 1B and data not shown). Activin βB expression was also induced by hypoxia in HCT116 colon cancer cells and human umbilical vein endothelial cells (HUVEC) (Fig. 1C). Efficient siRNA-mediated knockdown of HIF-1α and HIF-2α reduced expression of activin βB in HCT116 cells stimulated by hypoxia (Fig. 1D) and constitutive expression in RCC4 cells (Fig. 1E and data not shown). Expression of known HIF targets Glut-1 and CAIX was similarly reduced (Fig. 1D and E). In order to identify binding sites for HIF in the human activin βB promoter, we performed ChIP experiments. We found that a fragment from bp −4121 to −3917 upstream of the ATG start codon specifically precipitated with antibodies to HIF-2α in 786.0 cells but not with control antibodies or antibodies to HIF-1α, which is not expressed in these cells. The precipitated band was strongly reduced in 786.0 VHL cells, indicating that it depends on the presence of HIF proteins (Fig. 2A). Moreover, the fragment was precipitated with antibodies to both HIF-1α and HIF-2α in RCC4 cells, which express both factors. Again, precipitation was reduced to background levels in VHL transfectants (Fig. 2A). We cloned this fragment, which contains three HIF-responsive elements (HRE1 to HRE3) in front of the bp −1460 rat activin βB promoter coupled to luciferase (Fig. 2B). Reporter activity of this construct was enhanced by cotransfection of HIF-1α and HIF-2α, and mutation of HRE-1 but not of HRE-2 and HRE-3 strongly reduced activation by both HIFs. The rat promoter alone was weakly activated by HIFs under these conditions (Fig. 2C). We conclude that the human activin βB promoter region can bind HIF-1α and HIF-2α and is directly regulated by these factors on specific HREs.

In line with activin B being a target of VHL, activin βB mRNA was highly upregulated in RCC compared to levels in normal kidney tissue, as shown by qualitative and quantitative RT-PCR analyses (Fig. 3A and B). Upregulation of activin βB correlated with immunohistochemistry for HIF-1α and with upregulation of the known HIF target IGFBP3 (Fig. 3C and data not shown) (14). The activin βA mRNA was not regulated by VHL in the RCC cell lines as analyzed by RT-PCR and was rarely found to be expressed in tumors on microarrays. The inhibin α subunit was detected neither in cell lines nor in tumors by microarray analysis (data not shown).

Activin B mediates defects of cell matrix adhesion induced by loss of VHL. VHL transfectants of 786.0 and RCC4 cell lines showed more-efficient attachment to plastic culture dishes and a drastic increase in attachment to laminin-1-coated dishes compared with the VHL-deficient parental cells (Fig. 4A and B). Similar but smaller differences in attachment levels were also observed for fibronectin, collagen I, and collagen IV (Fig. 4B and data not shown). Importantly, pretreatment with recombinant activin B strongly reduced the matrix attachment of VHL transfectants (Fig. 4B). We generated stable clones of 786.0 cells expressing two different activin B shRNAs, namely, si1-βB#1 and -#2 and si2-βB#1 to -#3, which resulted in the efficient knockdown of activin B (Fig. 4E and F). These cells exhibited a strong increase in the attachment to laminin-1 and a moderate increase in the attachment to plastic, fibronectin, collagen I, and collagen IV compared to results with neo control clones (Fig. 4C and D and data not shown). Thus, activin B knockdown resulted in relative increases in cell attachment

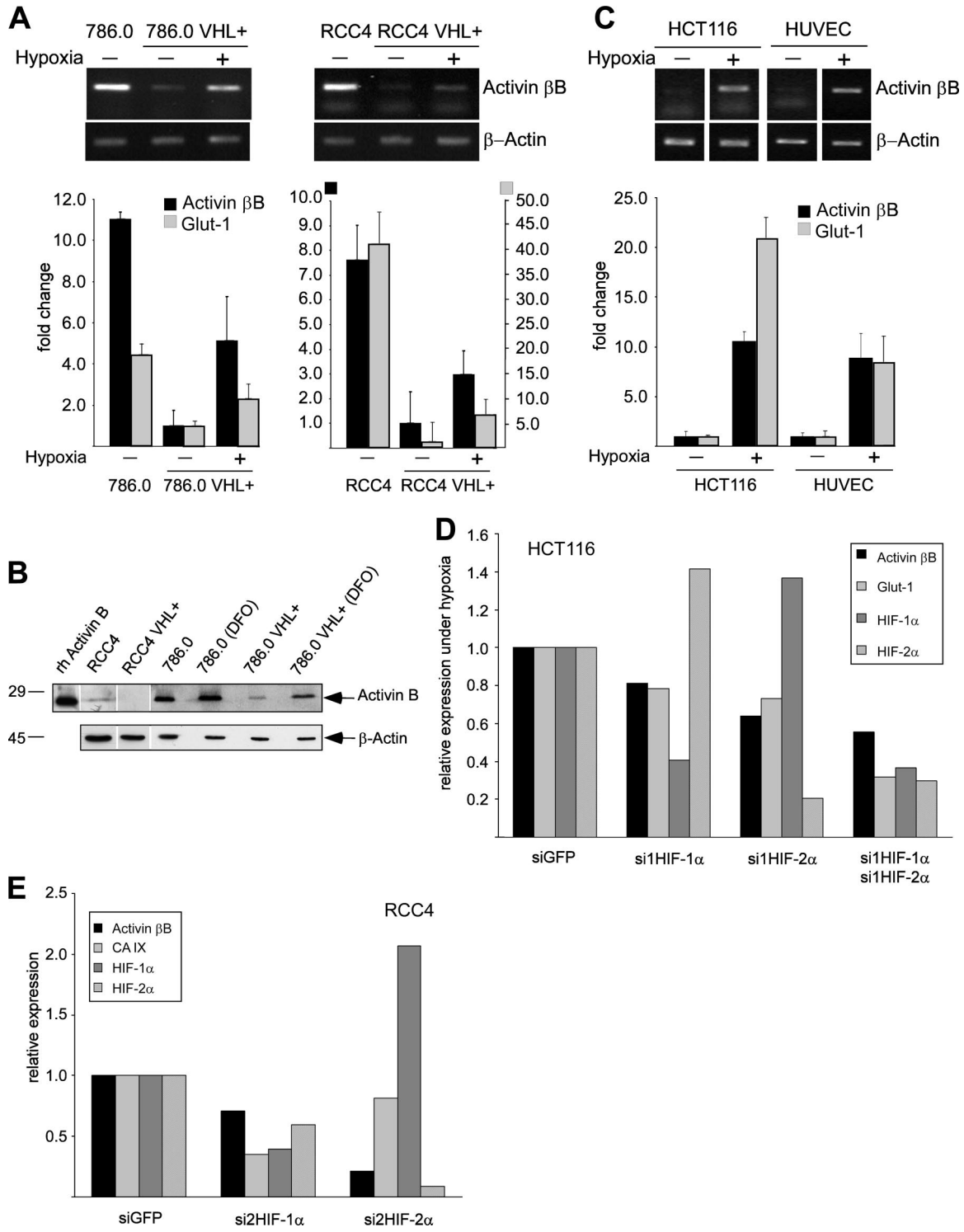

FIG. 1. Activin B expression is downregulated by VHL and upregulated by hypoxia. (A) Qualitative (upper panels) and quantitative (bar graph; $n = 3$) RT-PCR analysis for activin βB mRNA in VHL-deficient 786.0 and RCC4 parental cell lines and stable transfectants expressing wild-type VHL (VHL+) kept under normoxia (−) or hypoxia (+) for 16 h. The HIF target Glut-1 was analyzed as a positive control. (B) Western blot detection of activin B in cell supernatants collected from indicated cell lines and of recombinant human activin B (rh Activin B). Western blotting of β-actin from cell extracts of the same cultures was used to control for similar cell numbers. DFO, treatment with DFO for 16 h. (C) Qualitative (upper panels) and quantitative (bar graph; $n = 3$) RT-PCR analysis for the activin βB mRNA from HCT116 colon cancer cells and HUVEC kept under normoxia (−) or hypoxia (+) for 16 h. The HIF target Glut-1 was analyzed as a positive control. (D) Quantitative RT-PCR analysis for the activin βB, Glut-1, HIF-1α, and HIF-2α mRNAs in HCT116 cells transfected with siGFP (as a negative control) or siRNAs against HIF-1α (si1HIF-1α) and/or HIF-2α (si1HIF-2α). Cells were kept under hypoxia for 16 h after siRNA transfection. Results were normalized to the expression of β-actin and siGFP. (E) Quantitative RT-PCR analysis for the activin βB, CA IX, HIF-1α, and HIF-2α mRNAs in RCC4 cells transfected with siGFP (as a negative control) and siRNAs against HIF-1α and HIF-2α. Results were normalized to the expression of β-actin and siGFP. Note that siRNA against HIF-2α was more efficient than siRNA against HIF-1α. Similar results were obtained with a second, unrelated set of siRNAs to HIF-1α and HIF-2α.

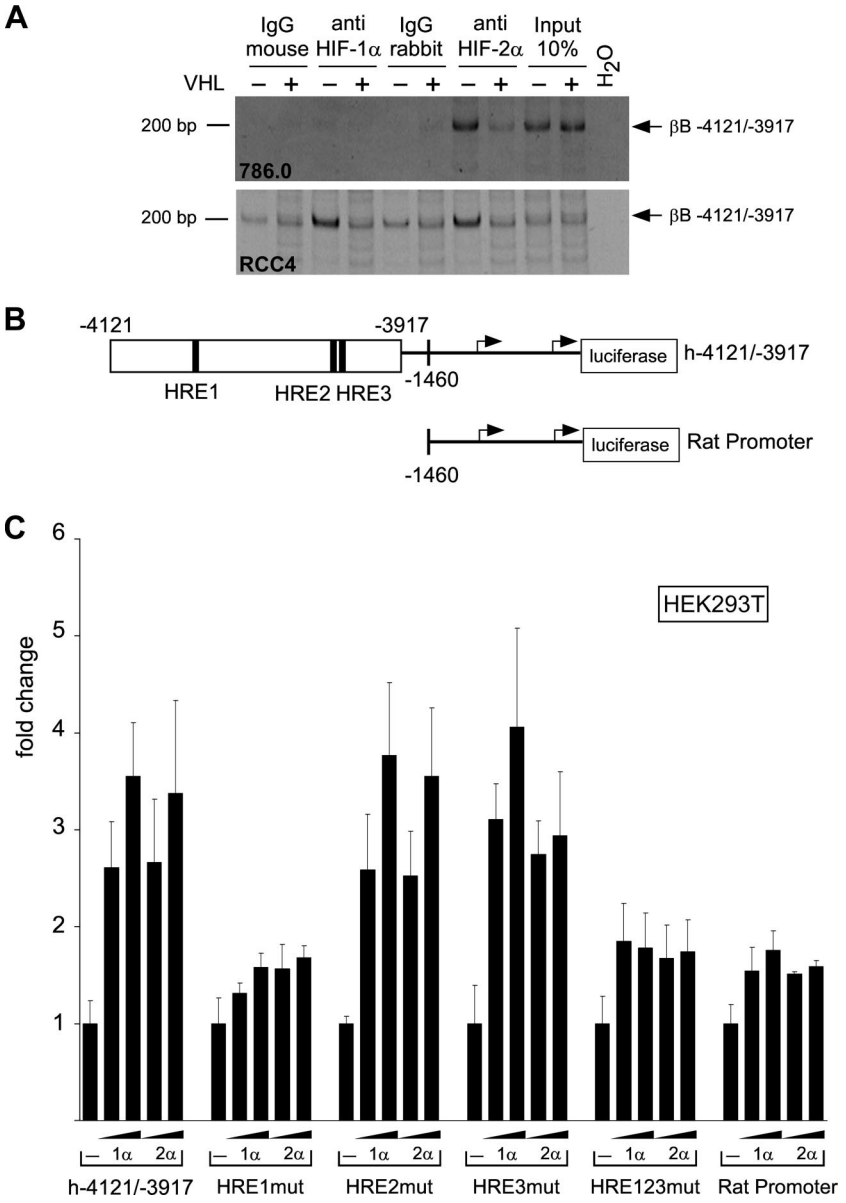

FIG. 2. Activin βB is a direct target of HIF. (A) ChIP analysis of 786.0 and RCC4 cells (VHL−) and VHL transfectants (VHL+) using anti-HIF-1α and anti-HIF-2α antibodies as indicated. Immunoglobulin G (IgG) was used as a control. Panels show PCR for a fragment of the activin βB promoter from bp −4121 to −3917 relative to the ATG start codon. (B) Scheme of activin βB promoter reporter constructs. The black boxes represent putative HREs, and the numbers denote positions relative to the ATG start codon. The arrows denote transcription start sites. (C) Induction of the indicated activin βB promoter reporter constructs by cotransfection of a HIF-1α or a HIF-2α expression plasmid, respectively. "mut" denotes individual or collective mutation of the HRE1 to HRE3 sites in h-4121/-3917.

to the various substrates that were similar to those seen with VHL transfection. Attachment of activin B knockdown cells was decreased again by treatment with recombinant activin B, ruling out unspecific effects of the introduced siRNA (Fig. 4F and data not shown). Activin B did not affect the viability of cells, as determined by an MTT assay (data not shown). Altogether, the data strongly argue that defects in cell matrix attachment of VHL-deficient cells are a consequence of the upregulation of activin B.

Activin B mediates cell shape changes induced by loss of VHL. After initial attachment to tissue culture dishes, 786.0 cells showed a conspicuous morphology with multiple cellular processes projecting from the cell center (Fig. 5A), which were enriched at their ends in integrin β1 and actin (Fig. 5B). In contrast, VHL transfectants were more flattened and round (Fig. 5A), and integrin β1 and actin were located in a thin rim at the edge of the cells, resembling lamellipodia (Fig. 5B). Remarkably, the morphology of activin B knockdown clones of 786.0 (shown for 786.0 si1-βB#1) completely matched that of the VHL transfectants; i.e., cells were flat, and integrin β1 and actin exhibited the rim pattern (Fig. 5B). Moreover, when treated with recombinant activin B, activin B knockdown cells

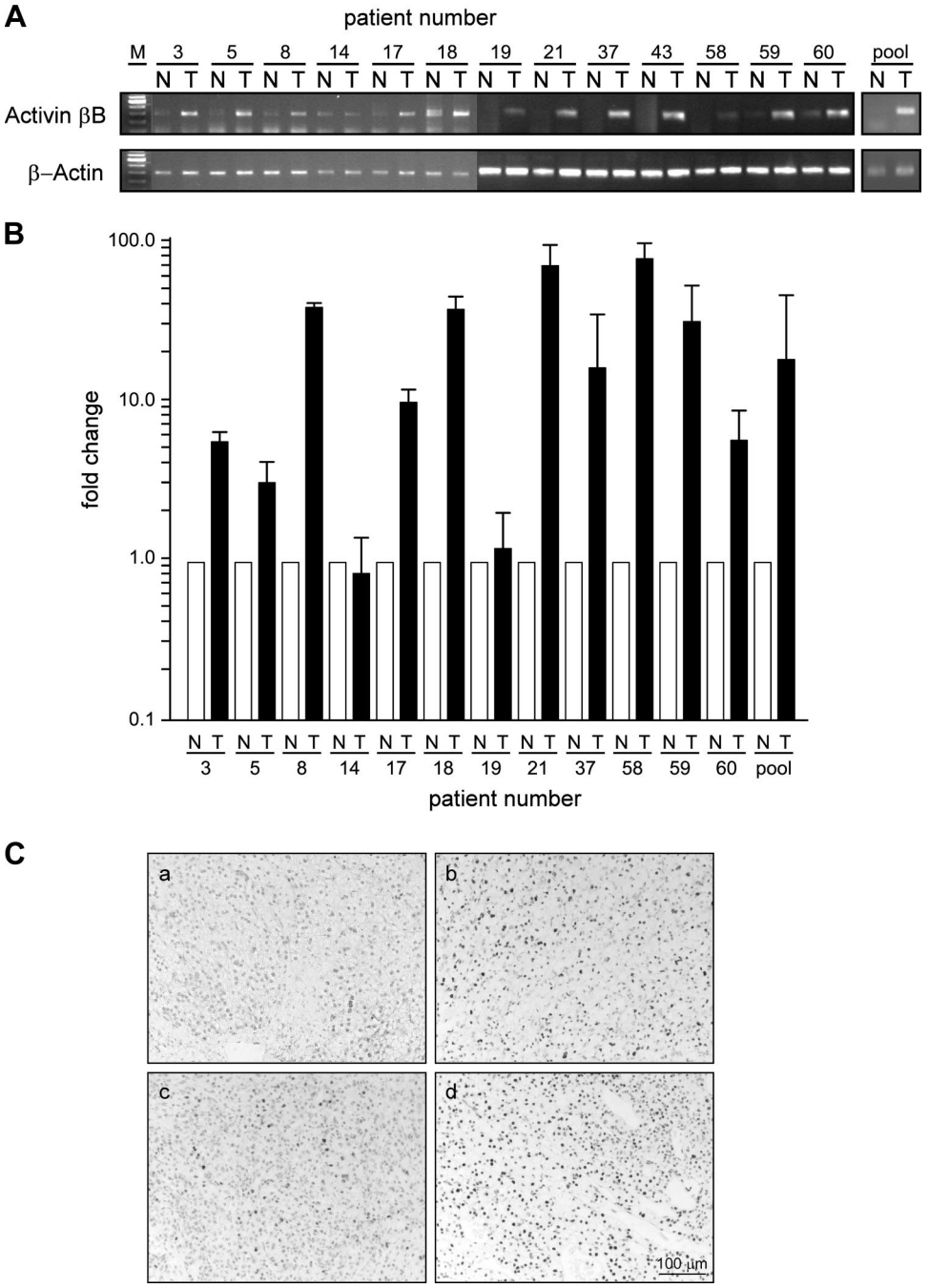

FIG. 3. Activin B expression is upregulated in clear cell RCC compared to levels in the normal kidney. (A) RT-PCR analysis of activin βB mRNA from clear cell RCC (T) or the corresponding human normal kidney (N) sample from the same patient. pool, pooled mRNA from the normal and tumor tissues used to produce cDNA. (B) Quantitative RT-PCR analysis of activin βB mRNA from clear cell RCC (T) or the corresponding human normal kidney (N) sample from the same patient. Results were normalized to the expression of β-actin. (C) Immunohistochemistry of HIF-1α on paraffin sections (a, b, c, and d, samples from patients 14, 3, 58, and 59, respectively).

and VHL transfectants reacquired the characteristic morphology of the parental cells (Fig. 5A and B). These data show that morphological differences between VHL-deficient cells and VHL transfectants are due to differences in activin B expression.

Activin B mediates invasiveness induced by loss of VHL. When plated on collagen I gels, RCC4 and 786.0 cells had a spindle-like shape and rarely appeared in clusters. In contrast, the VHL transfectants of RCC4 and 786.0 and the activin B knockdown cells of 786.0 were more spread out and frequently formed clusters, apparently exhibiting increased cell-cell contact formation (Fig. 6A). Importantly, the VHL-deficient cells efficiently invaded the collagen gel over a period of 3 to 5 days, whereas invasion was strongly impaired in VHL transfectants

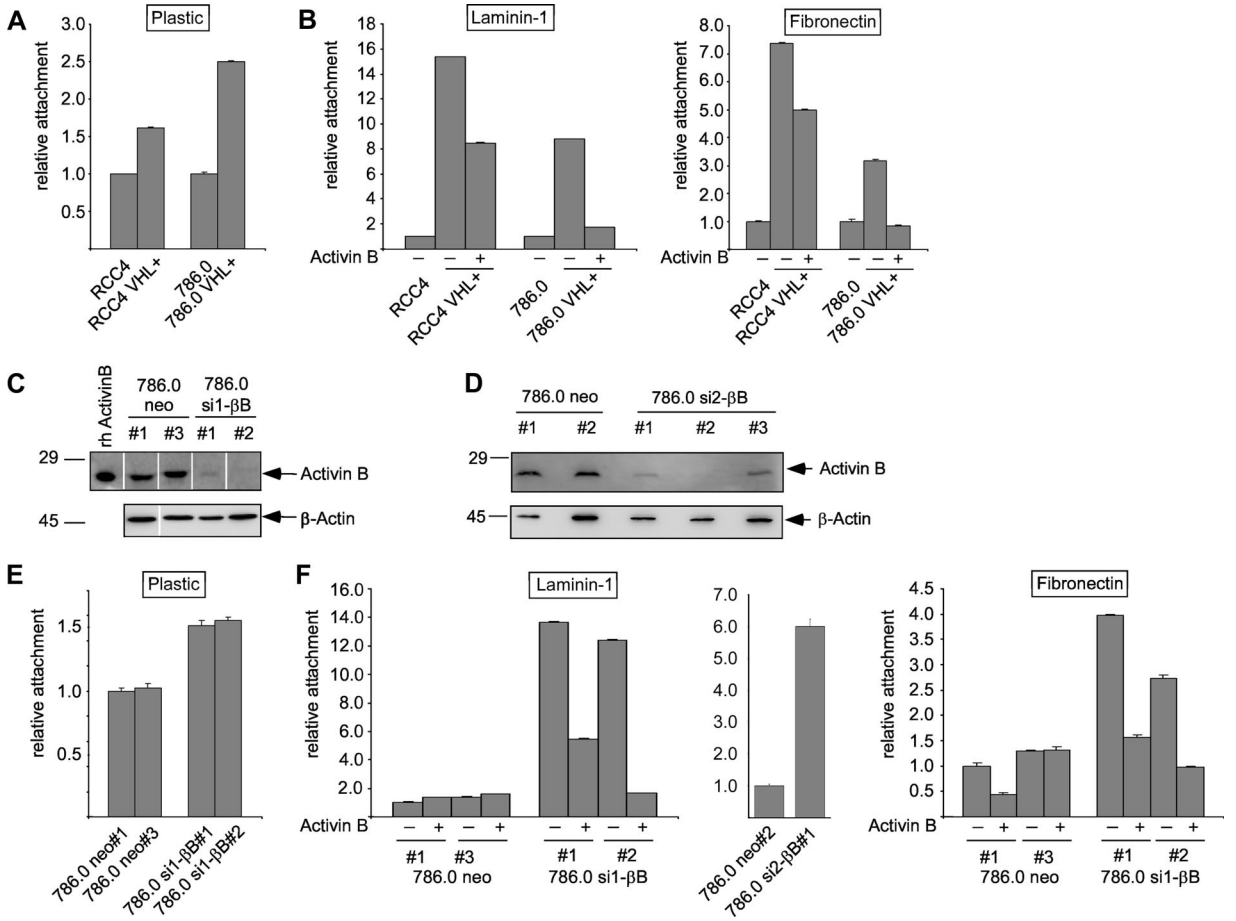

FIG. 4. VHL and knockdown of activin B by shRNA promotes cell attachment of RCC cell lines, which can be inhibited by activin B treatment (10 ng/ml). (A) Relative attachment of VHL-deficient 786.0 and RCC4 cell lines and stable transfectants expressing wild-type VHL (VHL+) to plastic culture dishes. (B) Relative attachment of cell lines as in panel A to culture dishes coated with laminin-1 or fibronectin. Cells were cultured without (−) or with (+) recombinant human activin B (10 ng/ml) for 1 week prior to the experiment. (C and D) Western blot detection of activin B in cell supernatants collected from transfectants carrying empty shRNA vector (neo#1 to neo#3) or two different shRNAs (sh1RNA and sh2RNA) targeting activin B (si1-βB#1 and si1-βB#2; si2-βB#1 to si2-βB#3), respectively. Rh activinB, recombinant human activin B. Western blotting of β-actin from cell extracts of the same cultures was used to control for similar cell numbers. (E) Relative attachment of cell lines as in panel C to plastic culture dishes. (F) Relative attachment of cell lines as in panels C and D to culture dishes coated with laminin-1 or fibronectin. Cells were cultured without (−) or with (+) recombinant human activin B (10 ng/ml) for 1 week prior to the experiment.

and activin B knockdown cells (Fig. 6B). In contrast, knockdown of activin B did not affect cell migration of 786.0 cells on plastic or collagen-coated wells, indicating that effects of activin B are specific for migration into three-dimensional matrices (data not shown). Pretreatment with recombinant activin B increased the invasiveness of the VHL transfectants as well as activin B knockdown cells by a factor of 3 to 4, whereas it had little effect on the invasion of VHL-deficient cells and neo control clones (Fig. 6C). Thus, activin B mediates invasiveness of RCC cells triggered by loss of VHL.

Knockdown of activin B in 786.0 cells reduces tumor growth in nude mice. To determine whether activin B has a role in tumor growth in vivo, we injected the si1-βB#2 and neo#1 cells, as well as a pool of si1-βB#1 to si1-βB#3 cells and a pool of neo#1 to neo#3 cells, subcutaneously into nude mice. After 12 weeks, large tumors had formed, with diameters ranging from 1.3 to 1.5 cm, in mice inoculated with neo control cells, a result in line with previous reports of 786.0 cells (15). In marked contrast, only small tumors, with diameters ranging from 0.4 to 0.7 cm, developed with the activin B knockdown cells (Fig. 7A). Growth curves show that the activin B knockdown cells were strongly restricted in tumor formation over the whole period of the experiment (Fig. 7B). Reduced tumor growth was also observed when a pool of the si2-βB clones (Fig. 4F) was injected (Fig. 7C). Knockdown of activin B did not affect cell proliferation of 786.0 cells in vitro as determined by counting cell numbers for 5 days (data not shown).

DISCUSSION

The VHL tumor suppressor controls a variety of cellular properties by downregulating the activity of HIF transcription factors and transcription of their target genes. Our data indicate that activin βB represents a direct target gene of HIF. A ChIP analysis shows binding of both HIF-1α and HIF-2α to the activin βB upstream regulatory region. This region contains

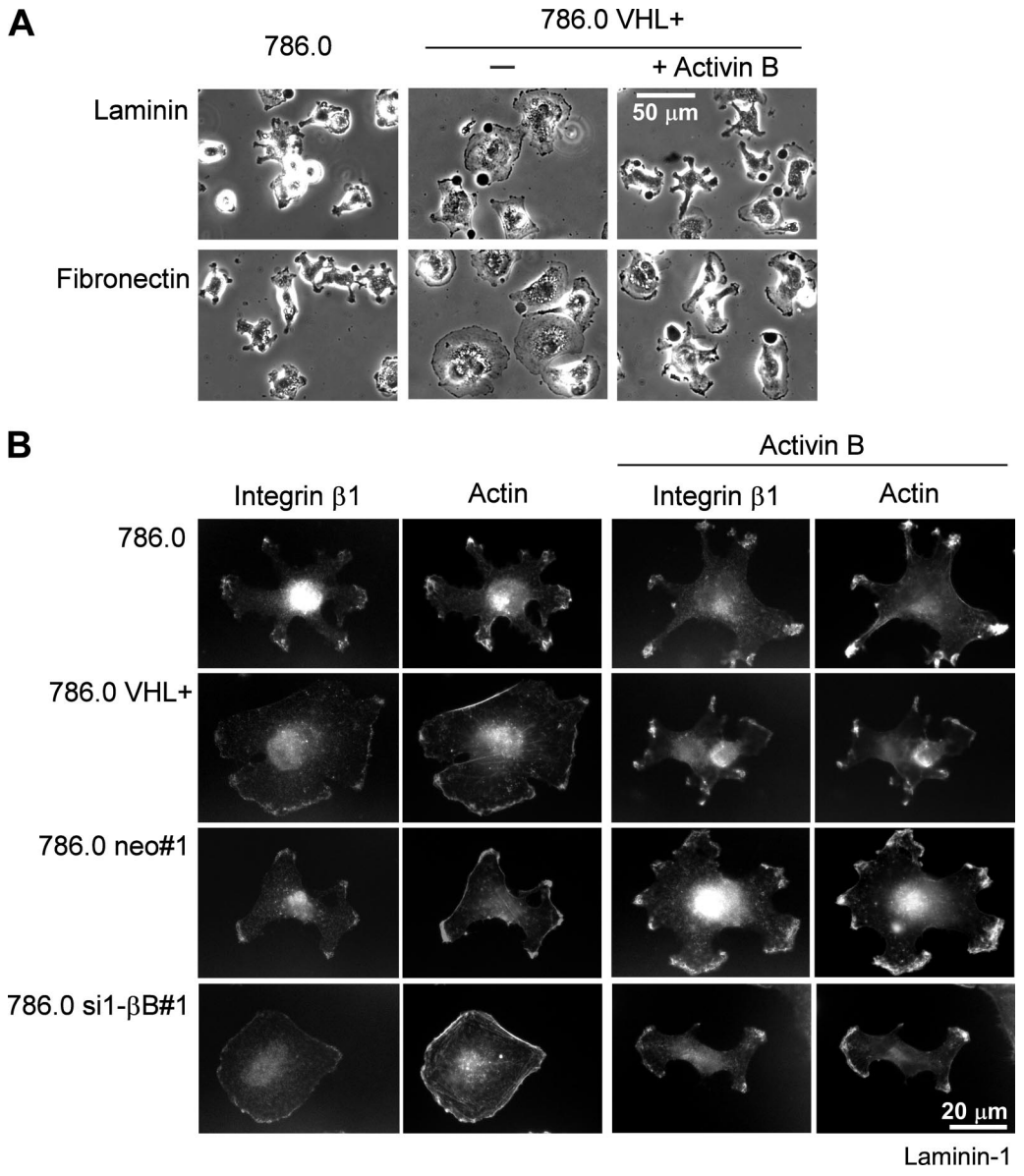

FIG. 5. Opposite changes in 786.0 cell morphology induced by VHL and activin B. (A) Phase-contrast image of VHL-deficient 786.0 and 786.0 cells transfected with wild-type VHL (786.0 VHL+) 1 h after plating to laminin-1 and fibronectin. Cells were cultured without (−) or with (+) recombinant human activin B (10 ng/ml) for 1 week prior to the experiment. (B) Double fluorescence staining for integrin β1 and actin of indicated cell lines plated on laminin-1 for 1 h. Where indicated, cells were cultured with activin B for 1 week prior to the experiment.

HREs, one of which was essential for conferring HIF inducibility to the promoter. In this study, we have analyzed three particular changes in cellular phenotype that result from VHL deficiency in RCC, namely, decreased adhesion to ECM, cell shape changes from a rounded to an elongated morphology, and increased invasiveness (7, 12, 18, 21, 26, 27). These features represent hallmarks of malignant transformation, and we provide conclusive evidence that all of them can be attributed to the upregulation of activin B after the loss of VHL. This conclusion is based on the findings that (i) the knockdown of activin B in VHL-deficient cells recapitulates phenotypic changes observed after reintroduction of wild-type VHL and (ii) exogenous activin B induced a VHL-deficient phenotype in the VHL transfectants and also reversed the effects of the activin B knockdown. Thus, we propose that VHL deficiency initiates an autocrine signaling loop via activin B that promotes the acquisition of malignant properties of the tumor cells.

A question arises as to how activin B induces the various phenotypic changes in RCC cells. The fact that activin B decreases adhesion to different substrates, although with various levels of efficiency, suggests that general regulators of cell adhesion are affected. For instance, activin B might induce proteases or change the cytoskeleton. Indeed, the actin cytoskeleton and the distribution of integrin β1 were altered by activin B in the 786.0 cells. It was recently shown that activin B can alter the cytoskeleton by modulating Rho signaling to induce keratinocyte migration (34, 35). However, a Rho kinase

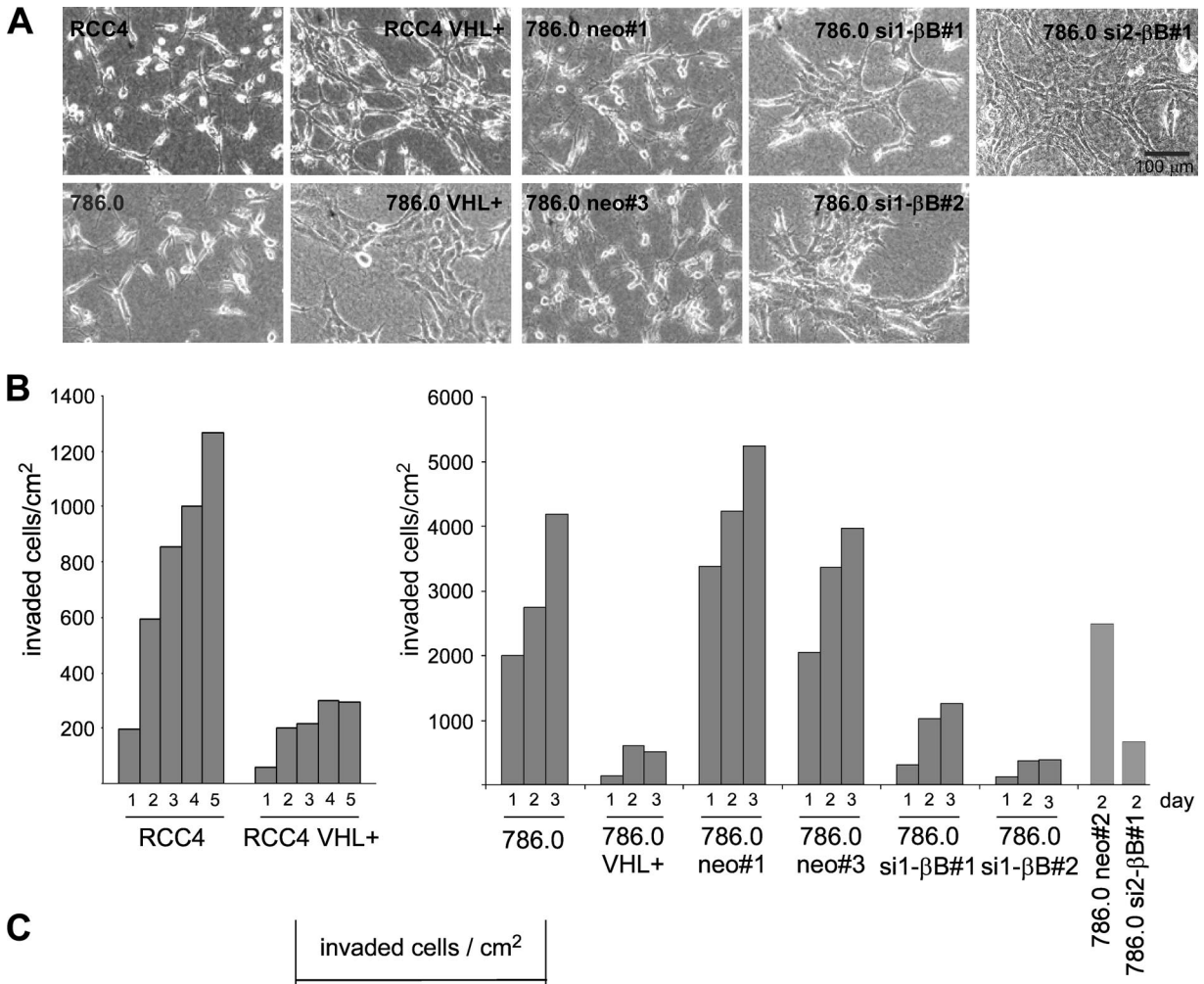

C

cell line	invaded cells / cm^2		fold change
	untreated	Activin B	
RCC4	1002	1758	1.75
RCC4 VHL+	297	701	2.36
786.0	4191	5803	1.38
786.0 VHL+	510	1465	2.87
786.0 neo#1	5242	5025	0.96
786.0 neo#3	3968	4904	1.23
786.0 si1-βB#1	586	1975	3.37
786.0 si1-βB#2	382	1490	3.90

FIG. 6. VHL and activin B promote changes in cell shape and invasiveness in RCC cells plated on collagen I gels. (A) Phase-contrast micrographs of indicated cell lines. (B) Invasiveness of indicated cell lines in collagen I gels at different time points (days) after plating. (C) Invasiveness of cell lines 3 days after plating when left untreated or treated with recombinant activin B (10 ng/ml) for 1 week prior to the experiment.

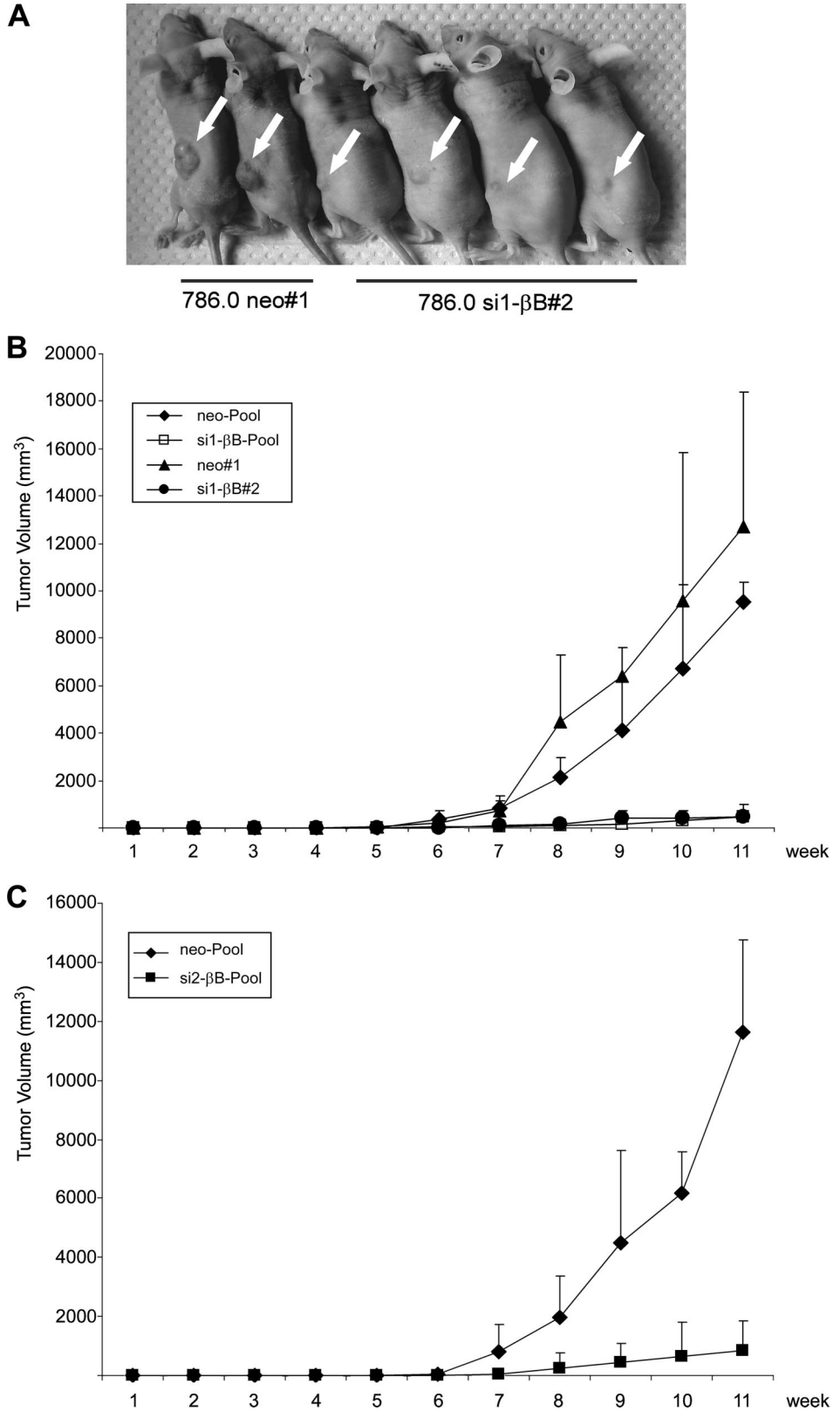

FIG. 7. Knockdown of activin B reduces growth of RCC cells in nude mice. Mice were injected with the cell lines indicated in Fig. 4. (A) Representative tumors formed 12 weeks after injection of 3×10^6 cells (arrows). (B) Increase in tumor volume of the indicated cell lines was determined over a period of 11 weeks (pool of clones neo#1 to neo#3, $n = 4$; clone neo#1, $n = 4$; pool of si1-βB#1 to si1-βB#3, $n = 4$; si1-βB#2, $n = 4$) (C) Increase in tumor volume of the indicated cell lines was determined over a period of 11 weeks (pool of neo#1 to neo#3, $n = 13$; pool of si2-βB#1 to si2-βB#3, $n = 7$). For panels B and C, 5×10^6 cells were injected.

inhibitor did not affect activin B-induced alterations in cell morphology and attachment (data not shown). It will be of interest to determine the molecular pathways underlying the activin B-dependent alterations in cell substrate adhesion and invasion of tumor cells.

Mutations of the VHL gene are common in both inherited and sporadic cases of RCC (2). We found upregulation of activin B expression in most of the clinical tumor samples analyzed, indicating that activin B signaling plays a role in the development or progression of this tumor type. Moreover, as activin B was also induced by hypoxia in colon tumor cells (HCT116) and in primary endothelial cells (HUVEC), it could well play a role in the pathogenesis of tumor types other than RCC, in particular under conditions of inadequate blood supply and hypoxia. Activin B also stimulated the invasion of breast cancer cell lines MDA MB 231 and MDA MB 436 (data not shown), and serum levels of activin A, which are closely related to activin B, correlate with the presence of bone metastasis from breast and prostate cancer (22).

Our xenograft experiments show that tumors formed from activin B knockdown cells are smaller than tumors from neo control clones. As we have not seen effects of activin B on cell proliferation and apoptosis in vitro, these results may come as a surprise. It is possible that growth of tumor cells in vivo is affected by activin B-dependent alterations in their cell-matrix interactions or that activin B has paracrine effects on stromal cells in the vicinity of the tumors, which may indirectly support tumor growth.

Activin B knockout mice, which show subtle phenotypes in eye and mammary gland development, have been generated (28, 31). Our study indicates that the animal models should be scrutinized for effects under hypoxic stress conditions. For example, both activin A and activin B have been implicated in wound healing, a process that is also influenced by oxygen tension. Altogether, the results of our study identify activin B signaling as a promising candidate for therapeutic interference of tumor development and progression associated with hypoxia and VHL deficiency.

ACKNOWLEDGMENTS

We thank P. Ratcliffe for providing the RCC4 and the RCC4 VHL+ cells, W. Kaelin for providing the 786.0 and the 786.0 VHL+ cells, K. von der Mark for gifts of reagents and for helpful discussions, and E. Schefler for technical assistance.

This work was supported by a grant from Sonderforschungsbereich 423 of the Deutsche Forschungsgemeinschaft to J.B.

REFERENCES

1. **Ananth, S., B. Knebelmann, W. Gruning, M. Dhanabal, G. Walz, I. E. Stillman, and V. P. Sukhatme.** 1999. Transforming growth factor beta1 is a target for the von Hippel-Lindau tumor suppressor and a critical growth factor for clear cell renal carcinoma. Cancer Res. **59:**2210–2216.
2. **Banks, R. E., P. Tirukonda, C. Taylor, N. Hornigold, D. Astuti, D. Cohen, E. R. Maher, A. J. Stanley, P. Harnden, A. Joyce, M. Knowles, and P. J. Selby.** 2006. Genetic and epigenetic analysis of von Hippel-Lindau (VHL) gene alterations and relationship with clinical variables in sporadic renal cancer. Cancer Res. **66:**2000–2011.
3. **Behrens, J., M. M. Mareel, F. M. Van Roy, and W. Birchmeier.** 1989. Dissecting tumor cell invasion: epithelial cells acquire invasive properties after the loss of uvomorulin-mediated cell-cell adhesion. J. Cell Biol. **108:** 2435–2447.
4. **Bellavite, P., G. Andrioli, P. Guzzo, P. Arigliano, S. Chirumbolo, F. Manzato, and C. Santonastaso.** 1994. A colorimetric method for the measurement of platelet adhesion in microtiter plates. Anal. Biochem. **216:**444–450.
5. **Brummelkamp, T. R., R. Bernards, and R. Agami.** 2002. A system for stable expression of short interfering RNAs in mammalian cells. Science **296:**550–553.
6. **Chen, Y. G., Q. Wang, S. L. Lin, C. D. Chang, J. Chuang, and S. Y. Ying.** 2006. Activin signaling and its role in regulation of cell proliferation, apoptosis, and carcinogenesis. Exp. Biol. Med. (Maywood) **231:**534–544.
7. **Davidowitz, E. J., A. R. Schoenfeld, and R. D. Burk.** 2001. VHL induces renal cell differentiation and growth arrest through integration of cell-cell and cell-extracellular matrix signaling. Mol. Cell. Biol. **21:**865–874.
8. **Deng, M., W. L. Chen, A. Takatori, Z. Peng, L. Zhang, M. Mongan, R. Parthasarathy, M. Sartor, M. Miller, J. Yang, B. Su, W. W. Kao, and Y. Xia.** 2006. A role for the mitogen-activated protein kinase kinase kinase 1 in epithelial wound healing. Mol. Biol. Cell **17:**3446–3455.
9. **Dykema, J. C., and K. E. Mayo.** 1994. Two messenger ribonucleic acids encoding the common beta B-chain of inhibin and activin have distinct 5′-initiation sites and are differentially regulated in rat granulosa cells. Endocrinology **135:**702–711.
10. **Erler, J. T., K. L. Bennewith, M. Nicolau, N. Dornhofer, C. Kong, Q. T. Le, J. T. Chi, S. S. Jeffrey, and A. J. Giaccia.** 2006. Lysyl oxidase is essential for hypoxia-induced metastasis. Nature **440:**1222–1226.
11. **Esteban, M. A., M. G. Tran, S. K. Harten, P. Hill, M. C. Castellanos, A. Chandra, R. Raval, S. T. O'Brien, and P. H. Maxwell.** 2006. Regulation of E-cadherin expression by VHL and hypoxia-inducible factor. Cancer Res. **66:**3567–3575.
12. **Esteban-Barragan, M. A., P. Avila, M. Alvarez-Tejado, M. D. Gutierrez, A. Garcia-Pardo, F. Sanchez-Madrid, and M. O. Landazuri.** 2002. Role of the von Hippel-Lindau tumor suppressor gene in the formation of beta1-integrin fibrillar adhesions. Cancer Res. **62:**2929–2936.
13. **Evans, A. J., R. C. Russell, O. Roche, T. N. Burry, J. E. Fish, V. W. K. Chow, W. Y. Kim, A. Saravanan, M. A. Maynard, M. L. Gervais, R. I. Sufan, A. M. Roberts, L. A. Wilson, M. Betten, C. Vandewalle, G. Berx, P. A. Marsden, M. S. Irwin, B. T. Teh, M. A. S. Jewett, and M. Ohh.** 2007. VHL promotes E2 box-dependent E-cadherin transcription by HIF-mediated regulation of SIP1 and Snail. Mol. Cell. Biol. **27:**157–169.
14. **Feldser, D., F. Agani, N. V. Iyer, B. Pak, G. Ferreira, and G. L. Semenza.** 1999. Reciprocal positive regulation of hypoxia-inducible factor 1alpha and insulin-like growth factor 2. Cancer Res. **59:**3915–3918.
15. **Iliopoulos, O., A. Kibel, S. Gray, and W. G. Kaelin, Jr.** 1995. Tumour suppression by the human von Hippel-Lindau gene product. Nat. Med. **1:**822–826.
16. **Kaelin, W. G., Jr.** 2002. Molecular basis of the VHL hereditary cancer syndrome. Nat. Rev. Cancer **2:**673–682.
17. **Kondo, K., W. Y. Kim, M. Lechpammer, and W. G. Kaelin, Jr.** 2003. Inhibition of HIF2alpha is sufficient to suppress pVHL-defective tumor growth. PLoS Biol. **1:**E83.
18. **Koochekpour, S., M. Jeffers, P. H. Wang, C. Gong, G. A. Taylor, L. M. Roessler, R. Stearman, J. R. Vasselli, W. G. Stetler-Stevenson, W. G. Kaelin, Jr., W. M. Linehan, R. D. Klausner, J. R. Gnarra, and G. F. Vande Woude.** 1999. The von Hippel-Lindau tumor suppressor gene inhibits hepatocyte growth factor/scatter factor-induced invasion and branching morphogenesis in renal carcinoma cells. Mol. Cell. Biol. **19:**5902–5912.
19. **Krishnamachary, B., S. Berg-Dixon, B. Kelly, F. Agani, D. Feldser, G. Ferreira, N. Iyer, J. LaRusch, B. Pak, P. Taghavi, and G. L. Semenza.** 2003. Regulation of colon carcinoma cell invasion by hypoxia-inducible factor 1. Cancer Res. **63:**1138–1143.
20. **Krishnamachary, B., D. Zagzag, H. Nagasawa, K. Rainey, H. Okuyama, J. H. Baek, and G. L. Semenza.** 2006. Hypoxia-inducible factor-1-dependent repression of E-cadherin in von Hippel-Lindau tumor suppressor-null renal cell carcinoma mediated by TCF3, ZFHX1A, and ZFHX1B. Cancer Res. **66:**2725–2731.
21. **Kurban, G., V. Hudon, E. Duplan, M. Ohh, and A. Pause.** 2006. Characterization of a von Hippel Lindau pathway involved in extracellular matrix remodeling, cell invasion, and angiogenesis. Cancer Res. **66:**1313–1319.
22. **Leto, G., L. Incorvaia, G. Badalamenti, F. M. Tumminello, N. Gebbia, C. Flandina, M. Crescimanno, and G. Rini.** 2006. Activin A circulating levels in patients with bone metastasis from breast or prostate cancer. Clin. Exp. Metastasis **23:**117–122.
23. **Maranchie, J. K., J. R. Vasselli, J. Riss, J. S. Bonifacino, W. M. Linehan, and R. D. Klausner.** 2002. The contribution of VHL substrate binding and HIF1-alpha to the phenotype of VHL loss in renal cell carcinoma. Cancer Cell **1:**247–255.
24. **Maxwell, P. H., M. S. Wiesener, G. W. Chang, S. C. Clifford, E. C. Vaux, M. E. Cockman, C. C. Wykoff, C. W. Pugh, E. R. Maher, and P. J. Ratcliffe.** 1999. The tumour suppressor protein VHL targets hypoxia-inducible factors for oxygen-dependent proteolysis. Nature **399:**271–275.
25. **Munz, B., H. Smola, F. Engelhardt, K. Bleuel, M. Brauchle, I. Lein, L. W. Evans, D. Huylebroeck, R. Balling, and S. Werner.** 1999. Overexpression of

activin A in the skin of transgenic mice reveals new activities of activin in epidermal morphogenesis, dermal fibrosis and wound repair. EMBO J. **18:** 5205–5215.
26. **Pennacchietti, S., P. Michieli, M. Galluzzo, M. Mazzone, S. Giordano, and P. M. Comoglio.** 2003. Hypoxia promotes invasive growth by transcriptional activation of the met protooncogene. Cancer Cell **3:**347–361.
27. **Peruzzi, B., G. Athauda, and D. P. Bottaro.** 2006. The von Hippel-Lindau tumor suppressor gene product represses oncogenic beta-catenin signaling in renal carcinoma cells. Proc. Natl. Acad. Sci. USA **103:**14531–14536.
28. **Robinson, G. W., and L. Hennighausen.** 1997. Inhibins and activins regulate mammary epithelial cell differentiation through mesenchymal-epithelial interactions. Development **124:**2701–2708.
29. **Schofield, C. J., and P. J. Ratcliffe.** 2004. Oxygen sensing by HIF hydroxylases. Nat. Rev. Mol. Cell Biol. **5:**343–354.
30. **Semenza, G. L.** 2003. Targeting HIF-1 for cancer therapy. Nat. Rev. Cancer **3:**721–732.
31. **Vassalli, A., M. M. Matzuk, H. A. Gardner, K. F. Lee, and R. Jaenisch.** 1994. Activin/inhibin beta B subunit gene disruption leads to defects in eyelid development and female reproduction. Genes Dev. **8:**414–427.
32. **Weiske, J., and O. Huber.** 2006. The histidine triad protein Hint1 triggers apoptosis independent of its enzymatic activity. J. Biol. Chem. **281:**27356–27366.
33. **Werner, S., and C. Alzheimer.** 2006. Roles of activin in tissue repair, fibrosis, and inflammatory disease. Cytokine Growth Factor Rev. **17:**157–171.
34. **Zhang, L., M. Deng, R. Parthasarathy, L. Wang, M. Mongan, J. D. Molkentin, Y. Zheng, and Y. Xia.** 2005. MEKK1 transduces activin signals in keratinocytes to induce actin stress fiber formation and migration. Mol. Cell. Biol. **25:**60–65.
35. **Zhang, L., W. Wang, Y. Hayashi, J. V. Jester, D. E. Birk, M. Gao, C. Y. Liu, W. W. Kao, M. Karin, and Y. Xia.** 2003. A role for MEK kinase 1 in TGF-beta/activin-induced epithelium movement and embryonic eyelid closure. EMBO J. **22:**4443–4454.